Solar Energy Materials & Solar Cells 95 (2011) 3377–3384

Contents lists available at ScienceDirect

Solar Energy Materials & Solar Cells

journal homepage: www.elsevier.com/locate/solmat

Development of DA-type polymers with phthalimide derivatives as electron withdrawing units and a promising strategy for the enhancement of photovoltaic properties

Jang Yong Lee [a], Kwan Wook Song [a], Ja Ram Ku [a], Tae Hyun Sung [b], Doo Kyung Moon [a,*]

[a] Department of Materials Chemistry and Engineering, Konkuk University, 1 Hwayang-dong, Gwangjin-gu, Seoul 143-701, Republic of Korea
[b] Department of Electrical Engineering, Hanyang University, 17 Haendang-dong, Seongdong-gu, Seoul 133-791, Republic of Korea

ARTICLE INFO

Article history:
Received 22 April 2011
Received in revised form
16 July 2011
Accepted 28 July 2011
Available online 10 August 2011

Keywords:
Organic photovoltaics
Phthalimide
Conjugated polymers
Copolymerization

ABSTRACT

We report on two push–pull type polymer semiconductors involving phthalimide derivatives as electron withdrawing units. The solubility and energy level of phthalimide could be easily controlled by introducing various functional groups in its nitrogen site. Additionally, the V_{OC} value of polymer semiconductor materials with phthalimide as an electron withdrawing unit could be efficiently enhanced because of the low HOMO energy level of phthalimide. Nevertheless, there are just a few of studies regarding the use of phthalimide in OPVs. In this study, we synthesized two photovoltaic polymer materials based on phthalimide with high V_{OC} value, PFTPT and PCTPT. Between the two polymers, PCTPT/$PC_{71}BM$-based photovoltaic cell afforded the best PCE value of 1.4% (V_{OC}=0.94 V, J_{SC}=4.41 mA/cm^2, FF=0.33) under 100 mW/cm^2 irradiation. In addition, a promising strategy for the development of high performance photovoltaic polymers with phthalimide derivatives as electron withdrawing units was investigated.

1. Introduction

Polymer semiconductors involving a variety of aromatic rings have been vigorously investigated for the past several decades because of their applications in organic electronics, such as organic photovoltaics (OPVs) [1–8], organic thin film transistors (OTFTs) [9–11], organic light emitting diodes (OLEDs) [12–15], etc. Particularly, OPVs have especially attracted significant research interest due to the worldwide technical trend towards sustainable development as well as a potential in fabricating low-cost integrated circuit elements for large area using various methods such as ink-jet printing and roll-to-roll through solution process [16–19].

From a materials point of view, the alternating donor–acceptor (DA) system has been regarded as the most effective method for developing organic photovoltaic materials, since polymer band gaps could be easily controlled by inducing orbital overlap between donor and acceptor materials [20,21]. However, there are a few of electron-donating and electron withdrawing candidate materials for high performance polymeric photovoltaic materials [22]. Particularly, since electron withdrawing materials have various restrictions, such as insolubility, electron affinity, instability, etc., the number of electron withdrawing materials is smaller compared to the number of electron-donating materials in DA-type polymers for organic photovoltaics. Nevertheless, the electronic and chemical properties of electron withdrawing moieties are very important parameters for determining that of polymers in DA-type copolymers.

Since the outstanding carrier mobility characteristic of polymer materials involving phthalimide was demonstrated for OTFTs [23], dicarboxylic imide-substituted thiophene and benzene have been attracted great attention due to their good n-type properties in OPVs. Recently, various photovoltaic materials with dicarboxylic imide-substituted thiophene (dioxopyrrolothiophene) have been reported [24–26], while there are no further studies concerning polymeric materials with dicarboxylic imide-substituted benzene (phthalimide) for OPVs [27].

Phthalimide derivatives have been vigorously investigated in organic electronics, such as OLEDs and OTFTs, because of their good electron withdrawing and π–π stacking properties [28]. One of the advantages of phthalimide is that its solubility and energy levels could be easily controlled by introducing various functional groups at the nitrogen site. Also, it is easy to efficiently enhance the open circuit voltage (V_{OC}) value of polymer semiconductor materials that involve phthalimide as an electron withdrawing unit, since the highest occupied molecular orbital (HOMO) energy level of phthalimide is lower than other typical electron withdrawing materials, such as benzothiadiazole, quinoxaline, oxadiazole, etc.

From this point of view, two DA-type polymer semiconductors that had a phthalimide derivative as an electron withdrawing

* Corresponding author. Tel.: +82 2 450 3498; fax: +82 2 444 0765.
E-mail address: dkmoon@konkuk.ac.kr (D.K. Moon).

0927-0248/$ - see front matter © 2011 Elsevier B.V. All rights reserved.
doi:10.1016/j.solmat.2011.07.033

moiety, poly[9,9-dioctylfluorene-co-5,5-(3,6-bis(thieno-2-yl)-N-(2-ethylhexyl))phthalimide] (PFTPT) and poly [N-9′-hepta-decanyl-2,7-carbazole-co-5,5-(3,6-bis(thieno-2-yl)-N-(2-ethylhexyl))phthalimide] (PCTPT), were synthesized through a Suzuki coupling reaction for organic photovoltaic materials. Bulk heterojunction-type devices with $PC_{61}BM$ and $PC_{71}BM$ as acceptors were fabricated in order to investigate the photovoltaic properties of PFTPT and PCTPT.

2. Experimental section

2.1. Instruments and characterization

All of the reagents and chemicals were purchased from Aldrich and used as received unless otherwise specified. The ^{1}H NMR (400 MHz) spectra were recorded using a Brüker AMX400 spectrometer in $CDCl_3$, and the chemical shifts were recorded in units of ppm with TMS as the internal standard. The elemental analyses were measured with EA1112 using a CE Instrument. The absorption spectra were recorded using an Agilent 8453 UV–vis spectroscopy system. The solutions that were used for the UV–vis spectroscopy measurements were dissolved in chloroform at a concentration of 10 μg/ml. The films were spin-coated from the chloroform solution onto a quartz substrate at a thickness of ca. 90 nm. All of the GPC analyses were carried out using THF as the eluent and a polystyrene standard as the reference. The TGA measurements were performed using a TA Instrument 2050. The cyclic voltammetric waves were produced using a Zahner IM6eX electrochemical workstation with a 0.1 M acetonitrile (substituted with nitrogen for 20 min) solution containing tetrabutyl ammonium hexafluorophosphate (Bu_4NPF_6) as the electrolyte at a constant scan rate of 50 mV/s. ITO, a Pt wire, and silver/silver chloride [Ag in 0.1 M KCl] were used as the working, counter, and reference electrodes, respectively. The electrochemical potential was calibrated against Fc/Fc^+. The HOMO levels of the polymers were determined using the oxidation onset value. Onset potentials are values obtained from the intersection of the two tangents drawn at the rising current and the baseline changing current of the CV curves. The LUMO levels were calculated from the differences between the HOMO energy levels and the optical band gaps, which were determined using the UV–vis absorption onset values in the films.

The current–voltage (*I–V*) curves of the photovoltaic devices were measured using a computer-controlled Keithley 2400 source measurement unit (SMU) that was equipped with a Peccell solar simulator under an illumination of AM 1.5 G (100 mW/cm^2). Thicknesses of the thin films were measured using a KLA Tencor Alpha-step 500 surface profilometer with an accuracy of 1 nm. Topographic images of the active layers were obtained through atomic force microscopy (AFM) in tapping mode under ambient conditions using a XE-100 instrument. Theoretical study was performed using density functional theory (DFT), as approximated by the B3LYP functional and employing the 6-31G* basis set in Gaussian09.

2.2. Fabrication and characterization of polymer solar cells

All of the bulk heterojunction PV cells were prepared using the following device fabrication procedure. The glass/indium tin oxide (ITO) substrates [Sanyo, Japan (10 Ω/γ)] were sequentially lithographically patterned, cleaned with detergent, and ultrasonicated in deionized water, acetone, and isopropyl alcohol. Then the substrates were dried on a hot-plate at 120 °C for 10 min and treated with oxygen plasma for 10 min in order to improve the contact angle just before the film coating process. Poly(3,4-ethylene-dioxythiophene): poly(styrene-sulfonate) (PEDOT:PSS, Baytron P 4083 Bayer AG) was passed through a 0.45 μm filter before being deposited onto ITO at a thickness of ca. 32 nm by spin-coating at 4000 rpm in air and then it was dried at 120 °C for 20 min inside a glove box. Composite solutions with polymers and PCBM were prepared using 1,2-dichlorobenzene (DCB). The concentration was controlled adequately in the 0.5 wt% range, and the solutions were then filtered through a 0.45 μm PTFE filter and then spin-coated (500–2000 rpm, 30 s) on top of the PEDOT:PSS layer. The device fabrication was completed by depositing thin layers of BaF_2 (1 nm), Ba (2 nm), and Al (200 nm) at pressures of less than 10^{-6} torr. The active area of the device was 4 mm^2. Finally, the cell was encapsulated using UV-curing glue (Nagase, Japan). In this study, all of the devices were fabricated with the following structure: ITO glass/PEDOT:PSS/polymer:PCBM/BaF_2/Ba/Al/ encapsulation glass.

The illumination intensity was calibrated using a standard a Si photodiode detector that was equipped with a KG-5filter. The output photocurrent was adjusted to match the photocurrent of the Si reference cell in order to obtain a power density of 100 mW/cm^2. After the encapsulation, all of the devices were operated under an ambient atmosphere at 25 °C.

2.3. Materials

All reagents were purchased from Aldrich and were used without further purification. N-(2-ethylhexyl)-3,6-dibromophthalimide **2** [23], 2,2′-(9,9-dioctyl-9H-fluorene-2,7-diyl)bis(4,4,5,5-tetramethyl-1,3,2-dioxaborolane) **5** [29], 9-(heptadecan-9-yl)-2,7-bis(4,4,5,5-tetramethyl-1,3,2-dioxaborolan-2-yl)-9H-carbazole **6** [30] were prepared as described in the literature.

2.3.1. 3,6-Dibromophthalic anhydride ***1***

A mixture of phthalic anhydride (5.9 g, 40 mmol), oleum(20% free SO_3, 75 ml), bromine (13.4 g, 84 mmol) and silver sulfate (25 g, 80.2 mmol) was stirred at 70 °C for 24 h. After cooling to room temperature, precipitations were filtered off and washed by dichloromethane. The solution was washed with water and extracted with chloroform. The organic layer was concentrated via rotary evaporation to a brown solid. This brown solid was recrystallized twice from acetic acid to provide colorless crystals (1.4 g, 4.5 mmol). ^{1}H NMR ($CDCl_3$; 400 MHz; ppm) 7.81 (s, 2H). ^{13}C NMR ($CDCl_3$; 400 MHz; ppm) 159.15, 141.55, 131.10, 120.16.

2.3.2. 3,6-Bis(thieno-2-yl)-N-(2-ethylhexyl)phthalimide ***3***

Compound **2** (1.54 g, 3.7 mmol), 2-tributylstannylthiophene (3.03 g, 8.14 mmol) and $Pd(PPh_3)_2Cl_2$ (5 mol%) were dissolved in a mixture of THF (40 ml). The mixture was refluxed at 70 °C for 24 h. After cooling to room temperature, the organic layer was dried with Na_2SO_4 and was concentrated via rotary evaporation. The product was purified using column chromatography using dichloromethane/hexane (1:3, v/v) as the eluent. The product was obtained as bright green viscous oil. (1.3 g, 3.05 mmol). ^{1}H NMR ($CDCl_3$; 400 MHz; ppm) 7.77 (d, 2H), 7.76 (s, 2H), 7.46 (d, 2H), 7.17 (t, 2H), 3.5 (d, 2H), 1.83 (m, 1H), 1.34–1.26 (m, 8H), 0.92 (t, 3H) 0.87 (t, 3H). ^{13}C NMR ($CDCl_3$; 400 MHz; ppm) 167.28, 137.25, 135.80, 132.29, 130.01, 128.04, 127.73, 127.58, 42.25, 38.15, 30.47, 28.59, 23.87, 23.05, 14.14, 10.35.

2.3.3. 5,5′-dibromo-3,6-bis(thieno-2-yl)-N-(2-ethylhexyl) phthalimide ***4***

Compound 3 (1.3 g, 3.05 mmol) were dissolved to mixture of chloroform/acetic acid (1:1, v/v) at room temperature. NBS (1.14 g, 6.5 mmol) was added to the mixture. After 24 h, the mixture was poured to water and organic layer was extracted with chloroform. The organic layer was dried with Na_2SO_4 and was concentrated via rotary evaporation. The product was purified using column

chromatography using dichloromethane/hexane (1:3, v/v) as the eluent. The product was obtained as bright green viscous oil. (1.6 g, 2.7 mmol). ^{1}H NMR ($CDCl_3$; 400 MHz; ppm) 7.68 (s, 2H), 7.51 (d, 2H), 7.11 (d, 2H), 3.51 (d, 2H), 1.82 (m, 1H), 1.33–1.26 (m, 8H), 0.89 (t, 3H) 0.85 (t, 3H). ^{13}C NMR ($CDCl_3$; 400 MHz; ppm) 167.35, 138.50, 135.34, 131.45, 130.59, 130.38, 127.84, 115.07, 42.28, 38.18, 30.58, 28.55, 23.89, 23.05, 14.10, 10.45.

2.3.4. General polymerization method

Reaction monomers (0.688 mmol), $Pd(PPh_3)_4$ (1.5 mol%) and Aliquot 336 were dissolved in a mixture of toluene and an aqueous solution of 2 M K_2CO_3. The solution was refluxed for 48 h with vigorous stirring in nitrogen atmosphere, and then the excess amount of bromobenzene and phenylboronic acid were added and stirring continued for 3 h, respectively. The whole mixture was poured into methanol. The precipitate was filtered off, purified with acetone, hexane, chloroform in soxhlet.

2.3.5. PFTPT

Yellow orange powder (0.30 g, 54%). ^{1}H NMR ($CDCl_3$; 400 MHz; ppm) 0.82 (t, 6H), 0.93 (t, 3H), 0.96 (t, 3H), 1.04–1.25 (br, 24H), 1.26–1.45 (br, 8H), 1.89 (m, 1H), 2.08 (br, 4H), 3.66 (d, 2H), 7.49 (d, 2H), 7.65 (s, 2H), 7.69–7.8 (br, 4H), 7.89 (br, 4H). Anal. calcd for $C_{53}H_{63}N_1S_2O_2$: C, 78.58; H, 7.84; N, 1.73; S, 7.9; O, 3.95. Found: C, 78.44; H, 7.81; N, 1.74; S, 7.88; O, 3.97.

2.3.6. PCTPT

Yellow orange powder (0.41 g, 72%). ^{1}H NMR ($CDCl_3$; 400 MHz; ppm) 0.82 (t, 6H), 0.93 (t, 3H), 0.97 (t, 3H), 1–1.25 (br, 24H), 1.26–1.45 (br, 8H), 1.92 (m, 1H), 2.04 (m, 2H), 2.39 (m, 2H), 3.66 (d, 2H), 4.67 (m, 1H),7.49 (d, 2H), 7.65 (s, 2H), 7.69–7.8 (br, 4H), 7.89 (br, 4H). Anal. calcd for $C_{53}H_{64}N_2S_2O_2$: C, 77.15; H, 7.82; N, 3.39; S, 7.76; O, 3.89. Found: C, 76.97; H, 7.85; N, 1.82; S, 7.81; O, 3.97.

3. Results and discussion

3.1. Material synthesis

The synthesis process for the monomers and polymers is shown in Scheme 1. Fluorene or carbazole, both of which have low HOMO energy levels, were adopted as electron donors to achieve an enhanced V_{OC} property. A thiophene spacer was introduced into the polymer skeleton to decrease the band gap by enlarging the π-conjugation length and to diminish the steric hindrance between the electron-donating unit and the electron withdrawing moiety.

The number average molecular weight (M_n) and the weight average molecular weight (M_w) of PFTPT and PCTPT were 38.1, 128.0 kg/mol and 36.1, 132.8 kg/mol, respectively. Particularly, the polymers exhibited very high values of M_w. Even though a high molecular weight allows polymers to have a low band gap, it can also hinder the improvement of crystallinity in conjugated polymers [31]. The polymers had decomposition temperatures (T_d) of over 340 °C, which indicated that they exhibited good thermal stability, making them applicable for use in polymer solar cells and other optoelectronic devices. The results of the molecular weight measurements and thermal properties are shown in Table 1.

Table 1
Molecular weights and thermal properties.

Polymer	Yield (%)	M_n (kg/mol)	M_w (kg/mol)	PDI	T_d (°C)
PFTPT	54	38.1	128.0	3.36	396
PCTPT	72	36.1	132.8	3.68	340

Molecular weights and polydispersity indexes determined by GPC in THF on the basis of polystyrene calibration.

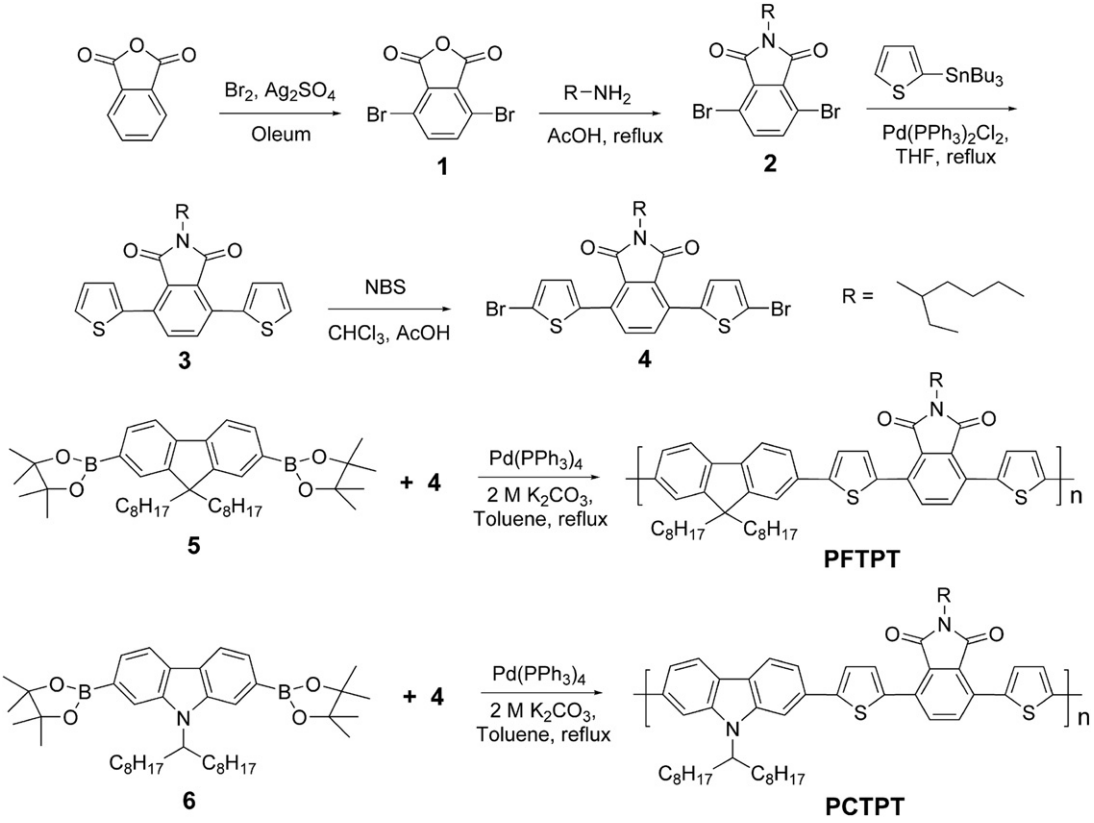

Scheme 1. Synthetic routes of PFTPT and PCTPT.

3.2. Optical and electrochemical properties

Figs. 1 and 2 show the UV–vis absorption and photoluminescence (PL) spectrum of PFTPT and PCTPT in the chloroform solution and in thin solid films, respectively. PFTPT exhibited maximum UV–vis absorption peaks (λ_{max}) at 428 nm in solution and 438 nm in film. PCTPT exhibited an almost identical λ_{max} as that of PFTPT. It is noteworthy that PCTPT had a much higher intensity of its UV–vis absorption peaks than did PFTPT in solution. Molecular absorption coefficients, calculated by Lambert law, of PFTPT and PCTPT were 3.89×10^3 and $2.16 \times 10^3\ M^{-1}\ cm^{-1}$, respectively. Since the difference of UV–vis absorption intensity indicates the difference of the amount of photons that an organic semiconductor can absorb from solar irradiation, and although PCTPT had an analogous UV–vis absorption spectrum range with PFTPT, it is estimated that PCTPT can absorb a larger amount of photons from the solar spectrum than PFTPT. UV–vis absorption data in films showed analogous results with those in solution. However, difference of absorption intensity in solution was smaller than in solution. It was because intermolecular interaction was increased in film. Furthermore, in Fig. 2, in comparison with PFTPT, PCTPT showed more red-shifted PL spectroscopy. It seemed that PCTPT had a stronger intermolecular interaction than PFTPT. Therefore, it is expected that PCTPT exhibits higher photovoltaic properties, especially its short circuit current density (J_{SC}) value, than PFTPT. The optical band gaps of PFTPT and PCTPT were calculated from the band edge of the UV–vis absorption spectrum in the film, and they were 2.40 and 2.36 eV, respectively.

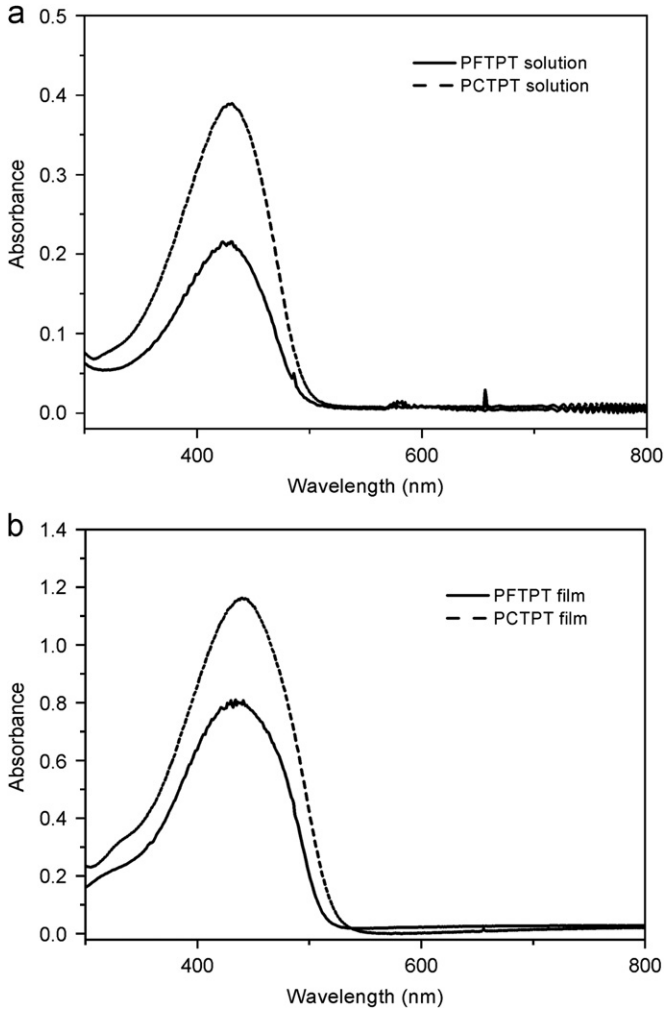

Fig. 1. Comparison of UV–vis absorption spectra of polymers (a) in solution (in chloroform at a concentration of 10 μg/ml), and (b) in film.

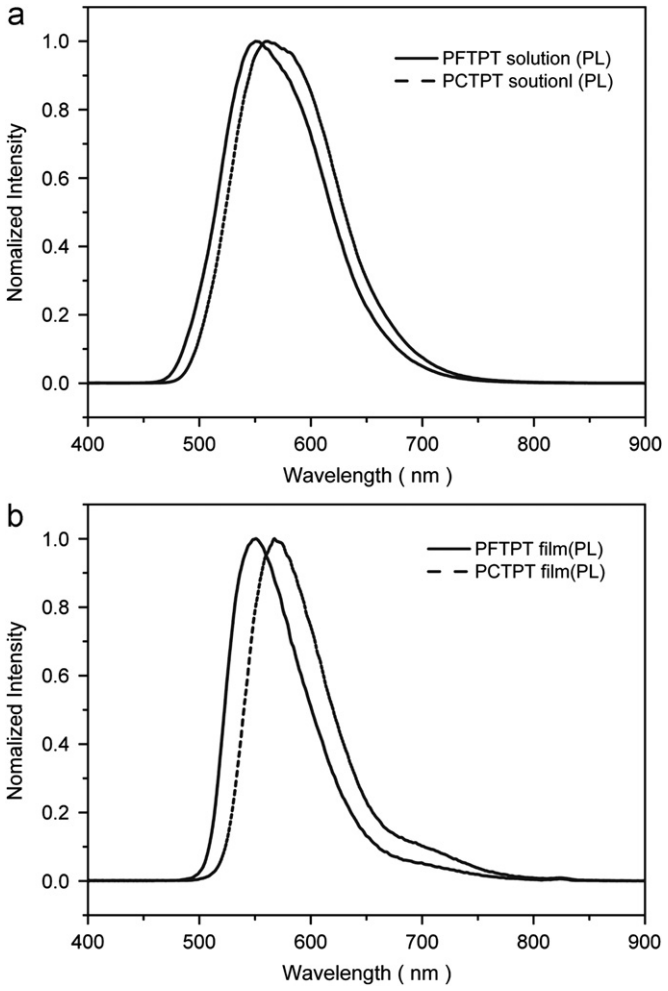

Fig. 2. Comparison of PL spectra of polymers (a) in solution (in chloroform), and (b) in film.

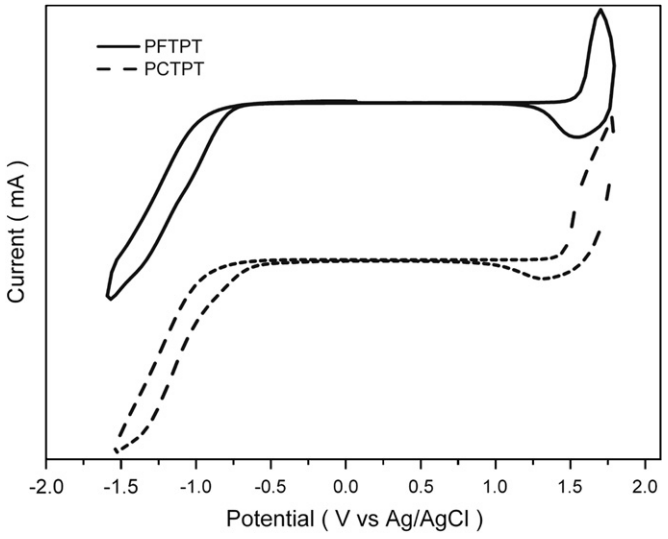

Fig. 3. Cyclic voltammograms of thin films recorded in 0.1 M Bu_4NPF_6/acetonitrile at a scan rate of 50 mV/s.

The electrochemical behavior of the copolymers was investigated using cyclic voltammetry (CV). The supporting electrolyte

was tetrabutyl ammonium hexafluorophosphate (Bu_4NPF_6) in acetonitrile (0.1 M), and the scan rate was 50 mV/s. The ITO glass and Pt plates were used as the working and counter electrodes, respectively, and silver/silver chloride (Ag in 0.1 M KCl) was used as the reference electrode. All of the other measurements were calibrated using the ferrocene value of −4.8 eV as the standard. The HOMO levels of the polymers were determined using the oxidation onset value. The lowest unoccupied molecular orbital (LUMO) levels were calculated from the differences between the HOMO energy levels and the optical band gaps, which were determined using the UV–vis absorption onset values in the films.

Fig. 3 shows the cyclic voltammograms of the synthesized polymers. The HOMO levels of PFTPT and PCTPT were −5.62 and −5.52 eV, respectively, and the LUMO levels were −3.26 and −3.12 eV, respectively. Taking note of the HOMO energy levels, it is expected that these polymers have high V_{OC} values as well as oxidative stability. [22] The low HOMO energy levels of the two polymers is likely not only due to the electron-donating materials, fluorene or carbazole, but they are also due to the electron withdrawing material, phthalimide, which has a low HOMO energy level. Considering that the V_{OC} value is determined by the difference between the HOMO level of the donor polymer and the LUMO level of the acceptor, it is expected that PFTPT and PCTPT will exhibit high V_{OC} values in the final device.

In spite of having ideal HOMO energy levels, the LUMO energy levels of the two were not low enough to transport electrons to the acceptor material (PCBM) in the bulk heterojunction photovoltaic device. This problem stemmed from the relatively high LUMO energy level of phthalimide. Considering that the LUMO energy level depends on the electron withdrawing material in the DA-type copolymer, it is supposed that the weak electron affinity of phthalimide had an effect on the LUMO energy levels of the polymers. The optical and electrochemical properties of the polymers are summarized in Table 2.

Table 2
Optical, electrochemical data, and energy levels of polymers.

Polymers	UV–vis absorption spectrum				PL emission spectrum		E_g^{op} (eV)[a]	Energy level (eV)	
	in $CHCl_3$		in film[b]		in $CHCl_3$	in film[b]		HOMO[c]	LUMO[d]
	λ_{max} (nm)	λ_{onset} (nm)	λ_{max} (nm)	λ_{onset} (nm)	λ_{max} (nm)	λ_{max} (nm)			
PFTPT	428	494	435	517	550	551	2.40	−5.62	−3.26
PCTPT	431	497	439	525	561	568	2.36	−5.52	−3.12

[a] Estimated from the onset of UV–vis absorption data of the thin film.
[b] Spin-coated from a chloroform.
[c] Calculated from the oxidation onset potentials under the assumption that the absolute energy level of Fc/Fc^+ was −4.8 eV below a vacuum.
[d] HOMO-E_g^{op}.

3.3. Morphology analysis

The morphologies of the polymer/PCBM blend films were examined using AFM. Surface interface morphology are very important factors that governed the device performance in the organic photovoltaics. In particular, the development of detailed p, n-channels has a decisive effect on the J_{SC} value and fill factor (FF). Dark-colored and light-colored areas correspond to PCBM domains and polymers, respectively, in Fig. 4. Although all of the blend films exhibited smooth surfaces, detailed polymer and $PC_{61}BM$-channels were not exhibited in polymer/$PC_{61}BM$ films, whereas the polymer/$PC_{71}BM$ blend films indicated more detailed p, n-channels than the polymer/$PC_{61}BM$ blend films. In other words, aggregated large $PC_{61}BM$ domains were shown in the polymer/$PC_{61}BM$ blend films, while detailed $PC_{71}BM$ domains were spread in the whole area. Since photoelectrons transfer to electrode through PCBM channels, development of detailed p, n-channels was very important factor. As shown in Fig. 4, the polymer/$PC_{71}BM$ (1/4, w/w) film had the best morphology among the fabricated films. On the basis of the above results, it was estimated that the device that had the PCTPT/$PC_{71}BM$ (1/4, w/w) blend film as an active layer would exhibit the best photovoltaic performance.

3.4. Photovoltaic characteristics

Fig. 5 illustrates the *I–V* properties of the fabricated devices. Bulk heterojunction solar cells using PFTPT and PCTPT as donor materials

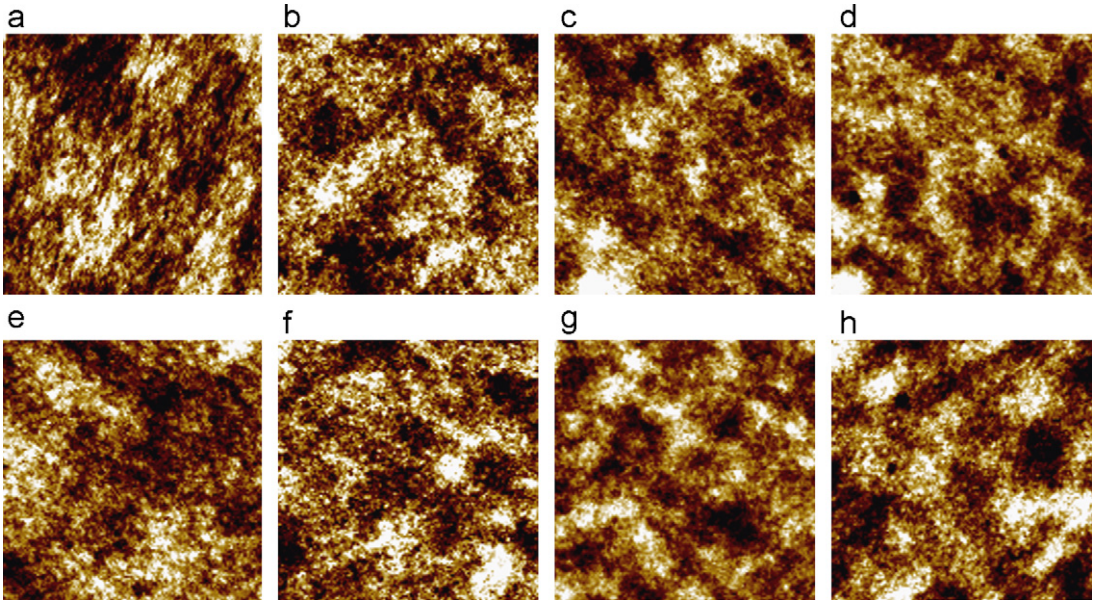

Fig. 4. AFM images of active layer films (1 nm × 1 nm): (a) PFTPT/$PC_{61}BM$ (1:3, w/w), (b) PFTPT/$PC_{61}BM$ (1:4, w/w), (c) PFTPT/$PC_{71}BM$ (1:3, w/w), (d) PFTPT/$PC_{71}BM$ (1:4, w/w), (e) PCTPT/$PC_{61}BM$ (1:3, w/w), (f) PCTPT/$PC_{61}BM$ (1:4, w/w), (g) PCTPT/$PC_{71}BM$ (1:3, w/w), and (h) PCTPT/$PC_{71}BM$ (1:4, w/w) blend films.

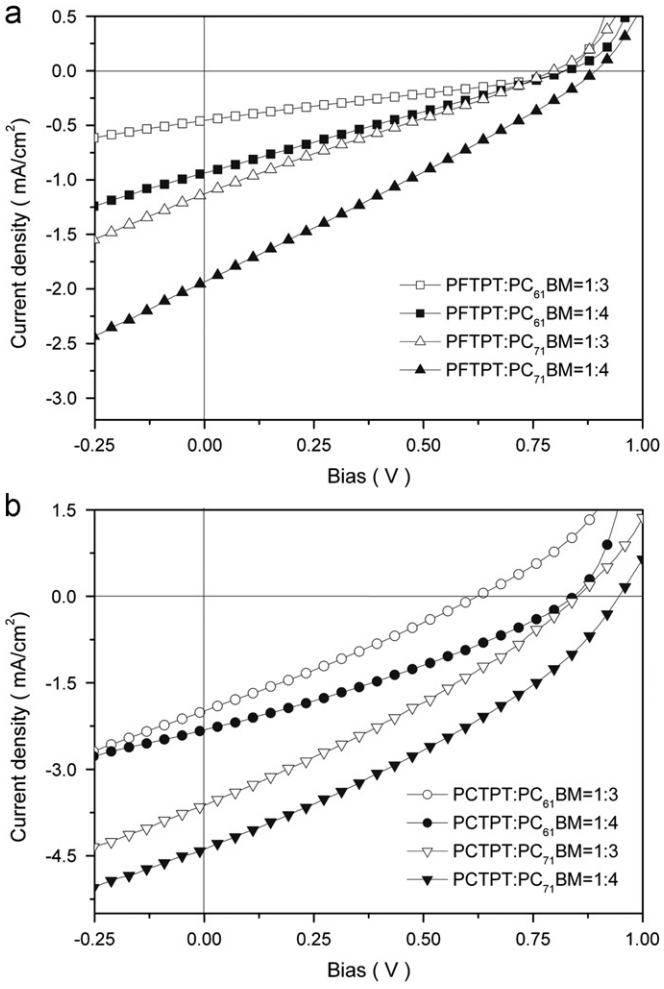

Fig. 5. *J–V* characteristics of photovoltaic devices with (a) PFTPT/PCBM and (b) PCTPT /PCBM blend films as active layers.

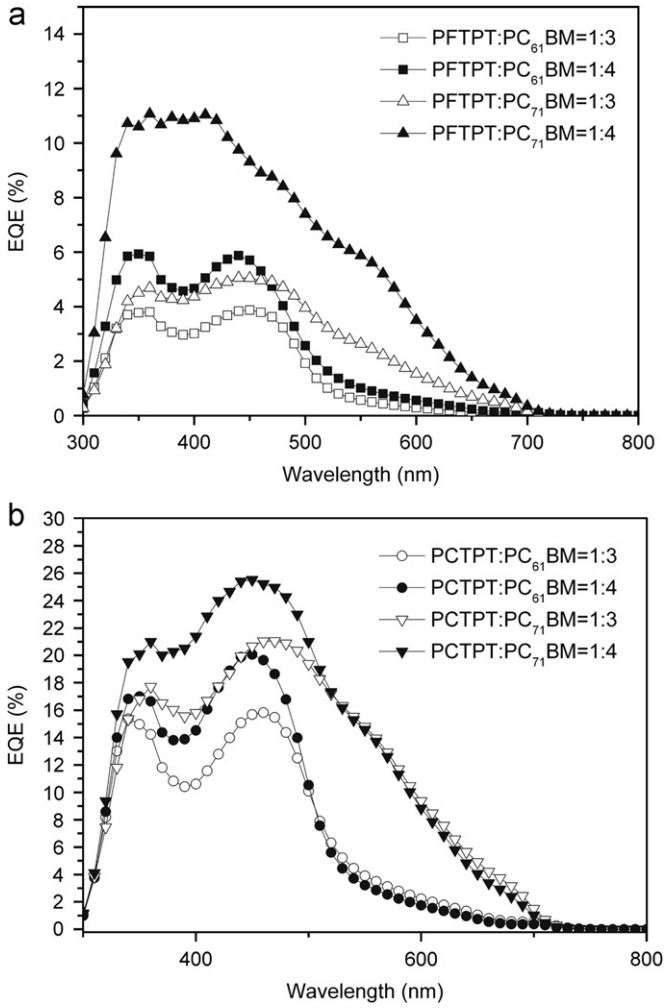

Fig. 6. EQE spectra of photovoltaic devices with (a) PFTPT/PCBM and (b) PCTPT / PCBM blend films as active layers.

and PCBM as an acceptor material were fabricated with a structure of ITO/PEDOT:PSS/polymer:PCBM/BaF_2/Ba/Al. Two sorts of PCBM, $PC_{61}BM$ and $PC_{71}BM$, were introduced as acceptor materials in order to confirm the acceptor effect in the polymer/PCBM blend. All the photovoltaic measurements were performed under 100 mW/cm^2 AM 1.5 sun illumination in ambient conditions.

PFTPT exhibited the best performance (0.90 V of V_{OC}, 1.9 mA/cm^2 of J_{SC}, 0.27 of FF, and 0.47% of power conversion efficiency (PCE)) in the device where 80 wt% $PC_{71}BM$ was contained in the active layer (pol:PCBM=1:4, w/w). PCTPT exhibited the best performance (0.94 V of V_{OC}, 4.4 mA/cm^2 of J_{SC}, 0.33 of FF, and 1.4% of PCE) under the same conditions. Upon comparing PFTPT with PCTPT, the difference of PCE resulted from the J_{SC} value. The difference of the J_{SC} value was explained by the EQE data (Fig. 6). PCTPT exhibited a much higher EQE value than did PFTPT in the same range of the solar spectrum. The difference of EQE between PFTPT and PCTPT correspond to the absorbance of UV–vis rays.

Although PFTPT and PCTPT exhibited high V_{OC} values of over 0.9 V, the PCE values of the two polymers were governed by their low J_{SC} values. There are two reasons why the two polymers exhibited low J_{SC} values. One reason is related to their large band gaps. They had relatively large band gaps of over 2.3 eV, which restrict photon harvesting. Upon considering that the largest amount of photons is in the range from 600 to 800 nm (from 2.1 to 1.5 eV), it was thought that their large band gaps (~2.4 eV) prohibited them from absorbing enough photons to achieve high J_{SC} values. Another reason for this was the low degree of intermolecular interaction. Strong intermolecular interactions not only lower polymer band gaps, but they also improve the mobility properties of holes and electrons. However, as shown in the UV–vis spectroscopy, they exhibited weak intermolecular interaction properties. From device fabrication technology viewpoint, the PCE values of the solar cells based on active materials with large band gaps can be improved in combination with up-converting devices [32]. However, as mentioned above, the most fundamental solution for high photovoltaic performance in organic solar cells is development of low band gap polymers with well-balanced energy levels.

In this point of view, if it solely focuses on the reduction of the band gap of polymer material for high PCE value, regardless of a balance between the HOMO energy level and the LUMO energy level, it is one method to introduce stronger electron-donating units, such as thiophene or fused thiophene units, instead of fluorene or carbazole, etc. However, in this case, since the HOMO energy level of the polymer will increase without decreasing the LUMO level, this strategy is not the best for maximizing the PCE value.

Thus, we suggest new strategies for synthesizing organic photovoltaic materials with phthalimide as an electron withdrawing unit. The strategy is to modify a phthalimide molecule. In other words, it is meant to improve electron affinity property of electron withdrawing material by introducing strong electron withdrawing functional groups, such as 3,4,5-trifluorobenzene, 3-trifluoromethylbenzene, etc, in phthalimide. For instance, according to

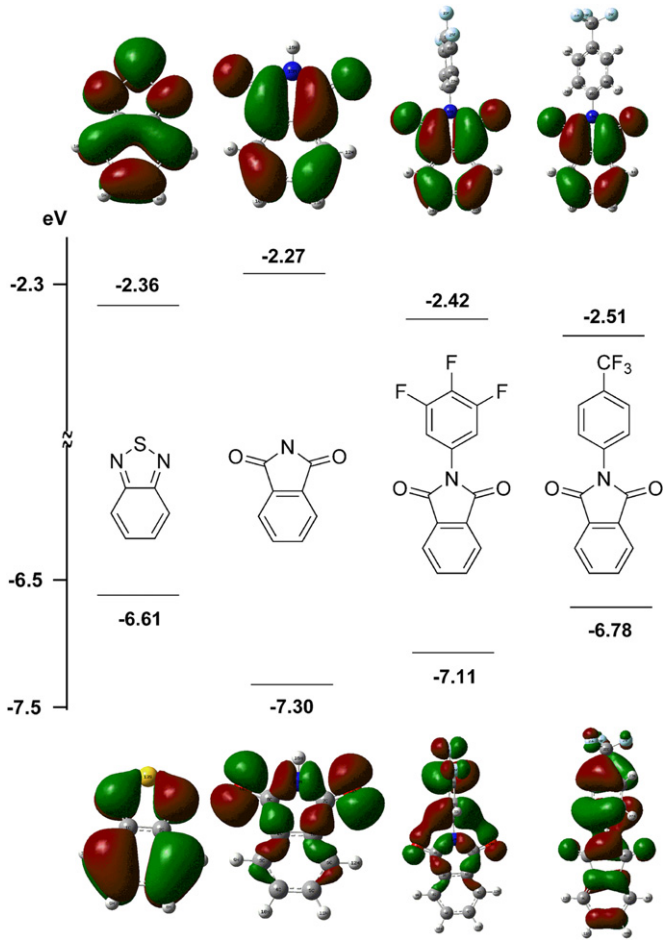

Fig. 7. Comparison of theoretical HOMO and LUMO energy levels between 2,1,3-benzothiadiazole and phthalimide derivatives.

Table 3
Summary of photovoltaic characteristics of devices.

Active layer (w/w)		Weight ratio (P:A, w/w)	V_{OC} (V)	J_{SC} (mA/cm^2)	FF	PCE (%)
Polymer (*P*)	Acceptor (*A*)					
PFTPT	$PC_{61}BM$	1:3	0.82	0.45	0.29	0.11
		1:4	0.82	0.93	0.26	0.19
	$PC_{71}BM$	1:3	0.80	1.10	0.26	0.23
		1:4	0.90	1.90	0.27	0.47
PCTPT	$PC_{61}BM$	1:3	0.62	2.01	0.28	0.34
		1:4	0.84	2.32	0.31	0.60
	$PC_{71}BM$	1:3	0.86	3.63	0.30	0.92
		1:4	0.94	4.41	0.33	1.40

a theoretical study (Fig. 7), a phthalimide derivative with 3,4,5-trifluorobenzene or 3-trifluoromethylbenzene, which is a strong electron withdrawing functional group, had a lower LUMO energy level than 2,1,3-benzothiadiazole. Nevertheless, its HOMO energy level was also lower than 2,1,3-benzothiadiazole. Moreover, since the hydrophobic property of the polymer could be enhanced by introducing fluorine atoms in the polymer skeleton, it is expected that the morphology, that is the detailed p, n-channel structure, of the polymer/PCBM blend film could also be improved.

Taking all of these results into account, if phthalimide derivatives with strong electron affinity properties are adopted as electron withdrawing units in polymer backbones, it is expected that these new photovoltaic materials will not only have high V_{OC} values, like PFTPT and PCTPT, but also high J_{SC} values. The photovoltaic properties of PFTPT and PCTPT are summarized in Table 3.

4. Conclusions

In summary, PFTPT and PCTPT, which are based on phthalimide, were successfully synthesized through the Suzuki coupling reaction for the OPVs. PFTPT and PCTPT had relatively wide band gaps of 2.40 and 2.36 eV, respectively, which prohibited them from absorbing photons in the large range of the solar spectrum. However, PFTPT and PCTPT had low HOMO energy levels, which resulted in the high V_{OC} values of the two polymers (0.90 and 0.94 eV, respectively). Although the two polymers did not exhibit very high PCEs, if phthalimide derivatives with reinforced electron affinity due to introducing electron withdrawing functional groups are adopted in polymer backbones, it is expected that new high performance organic photovoltaic materials will be developed.

Acknowledgments

This research was supported by a Grant from the Fundamental R&D Program for Core Technology of Materials funded by the Ministry of Knowledge Economy, Republic of Korea and the National Research Foundation of Korea Grant funded by the Korean Government (MEST) (NRF-2009-C1AAA001-2009-0093526).

References

[1] H. Bronstein, Z. Chen, R.S. Ashraf, W. Zhang, J. Du, J.R. Durrant, P.S. Tuladhar, K. Song, S.E. Watkins, Y. Geerts, M.M. Wienk, R.A.J. Janssen, T. Anthopoulos, H. Sirringhaus, M. Heeney, I. McCulloch, Thieno[3,2-b]thiophene-diketopyrrolopyrrole-containing polymers for high-performance organic field-effect transistors and organic photovoltaic devices, J. Am. Chem. Soc. 133 (2011) 3272–3275.
[2] K.H. Ong, S.L. Lim, H.S. Tan, H.K. Wong, J. Li, Z. Ma, L.C.H. Moh, S.H. Lim, J.C. de Mello, Z.K. Chen, A versatile low bandgap polymer for air-stable, high-mobility field-effect transistors and efficient polymer solar cells, Adv. Mater. 23 (2011) 1409–1413.
[3] G. Zhao, Y. He, C. He, H. Fan, Y. Zhao, Y. Li, Photovoltaic properties of poly(benzothiadiazole-thiophene-co-bithiophene) as donor in polymer solar cells, Sol. Energy Mater. Sol. Cells 95 (2011) 704–711.
[4] M. Manceau, E. Bundgaard, J.E. Carlé, O. Hagemann, M. Helgesen, R. Søndergaard, M. Jørgensen, F.C. Krebs, Photochemical stability of π-conjugated polymers for polymer solar cells: a rule of thumb, J. Mater. Chem. 21 (2011) 4132–4141.
[5] L. Huo, J. Hou, S. Zhang, H.Y. Chen, Y. Yang, A polybenzo[1,2-b:4,5-b′]dithiophene derivative with deep HOMO level and its application in high-performance polymer solar cells, Angew. Chem. Int. Ed. 49 (2010) 1500–1503.
[6] Y. Zou, A. Najari, P. Berrouard, S. Beaupré, B.R. Aïch, Y. Tao, M. Leclerc, A thieno[3,4-c]pyrrole-4,6-dione-based copolymer for efficient solar cells, J. Am. Chem. Soc. 132 (2010) 5330–5331.
[7] R.S. Ashraf, J. Gilot, R.A.J. Janssen, Fused ring thiophene-based poly(heteroarylene ethynylene)s for organic solar cells, Sol. Energy Mater. Sol. Cells 94 (2010) 1759–1766.
[8] J.Y. Lee, W.S. Shin, J.R. Haw, D.K. Moon, Low band-gap polymers based on quinoxaline derivatives and fused thiophene as donor materials for high efficiency bulk-heterojunction photovoltaic cells, J. Mater. Chem. 19 (2009) 4938–4945.
[9] Y. Li, P. Sonar, S.P. Singh, M.S. Soh, M. van Meurs, J. Tan, Annealing-free high-mobility diketopyrrolopyrrole-quaterthiophene copolymer for solution-processed organic thin film transistors, J. Am. Chem. Soc. 133 (2011) 2198–2204.
[10] P.M. Beaujuge, W. Pisula, H.N. Tsao, S. Ellinger, K. Müllen, J.R. Reynolds, Tailoring structure-property relationships in dithienosilole-benzothiadiazole donor–acceptor copolymers, J. Am. Chem. Soc. 131 (2009) 7514–7515.
[11] B.S. Ong, Y. Wu, Y. Li, P. Liu, H. Pan, Thiophene polymer semiconductors for organic thin-film transistors, Chem. Eur. J. 14 (2008) 4766–4778.
[12] J. Wang, C. Zhang, C. Zhong, S. Hu, X. Chang, Y. Mo, X. Chen, H. Wu, Highly efficient and stable deep blue light emitting poly(9,9-dialkoxyphenyl-2,7-silafluorene): synthesis and electroluminescent properties, Macromolecules 44 (2011) 17–19.
[13] J.Y. Lee, M.H. Choi, D.K. Moon, J.R. Haw, Synthesis of fluorene- and anthracene-based p-conjugated polymers and dependence of emission range and

luminous efficiency on molecular weight, J. Ind. Eng. Chem. 16 (2010) 395–400.
[14] K.S. Yook, J.Y. Lee, Origin of bistable memory characteristics of organic light-emitting diodes with LiF/Al cathode, J. Ind. Eng. Chem. 16 (2010) 230–232.
[15] S.O. Kim, H.C. Jung, M.J. Lee, C. Jun, Y.H. Kim, S.K. Kwon, Synthesis and characterization of 9,10-diphenylanthracene-based blue light emitting materials, J. Polym. Sci. Part A: Polym. Chem. 47 (2009) 5908–5916.
[16] F.C. Krebs, J. Fyenbo, M. Jørgensen, Product integration of compact roll-to-roll processed polymer solar cell modules: methods and manufacture using flexographic printing, slot-die coating and rotary screen printing, J. Mater. Chem. 20 (2010) 8994–9001.
[17] F.C. Krebs, T. Tromholt, M. Jørgensen, Upscaling of polymer solar cell fabrication using full roll-to-roll processing, Nanoscale 2 (2010) 873–886.
[18] F.C. Krebs, T.D. Nielsen, J. Fyenbo, M. Wadstrøm, M.S. Pedersen, Manufacture, integration and demonstration of polymer solar cells in a lamp for the Lighting Africa initiative, Energy Environ. Sci. 3 (2010) 512–525.
[19] F.C. Krebs, Polymer solar cell modules prepared using roll-to-roll methods: knife-over-edge coating, slot-die coating and screen printing, Sol. Energy Mater. Sol. Cells 93 (2009) 465–475.
[20] R. Kroon, M. Lenes, J.C. Hummelen, P.W.M. Blom, B. de Boer, Small bandgap polymers for organic solar cells (polymer material development in the last 5 years), Polym. Rev. 48 (2008) 531–582.
[21] E. Bundgaard, F.C. Krebs, Low band gap polymers for organic photovoltaics, Sol. Energy Mater. Sol. Cells 91 (2007) 954–985.
[22] N. Blouin, A. Michaud, D. Gendron, S. Wakim, E. Blair, R. Neagu-Plesu, M. Belletête, G. Durocher, Y. Tao, M. Leclerc, Toward a rational design of poly(2,7-carbazole) derivatives for solar cells, J. Am. Chem. Soc. 130 (2008) 732–742.
[23] X. Guo, F.S. Kim, S.A. Jenekhe, M.D. Watson, Phthalimide-based polymers for high performance organic thin-film transistors, J. Am. Chem. Soc. 131 (2009) 7206–7207.
[24] E. Zhou, J. Cong, K. Tajima, C. Yang, K. Hashimoto, Synthesis and photovoltaic properties of donor–acceptor copolymer based on dithienopyrrole and thienopyrroledione, Macromol. Chem. Phys. 212 (2011) 305–310.
[25] Y. Zhang, S.K. Hau, H.L. Yip, Y. Sun, O. Acton, A.K.Y. Jen, Efficient polymer solar cells based on the copolymers of benzodithiophene and thienopyrroledione, Chem. Mater. 22 (2010) 2696–2698.
[26] G. Zhang, Y. Fu, Q. Zhang, Z. Xie, Benzo[1,2-b:4,5-b′]dithiophene-dioxopyrrolothiophen copolymers for high performance solar cells, Chem. Commun. 46 (2010) 4997–4999.
[27] H. Xin, X. Guo, F.S. Kim, G. Ren, M.D. Watson, S.A. Jenekhe, Efficient solar cells based on a new phthalimide-based donor–acceptor copolymer semiconductor: morphology, charge-transport, and photovoltaic properties, J. Mater. Chem. 19 (2009) 5303–5310.
[28] H. Qu, J. Luo, X. Zhang, C. Chi, Dicarboxylic imide-substituted poly (p-phenylene vinylenes) with high electron affinity, J. Polym. Sci.: Part A: Polym. Chem. 48 (2010) 186–194.
[29] J.Y. Lee, Y.J. Kwon, J.W. Woo, D.K. Moon, Synthesis and characterization of fluorene- thiophene based π-conjugated polymers using coupling reaction, J. Ind. Eng. Chem. 14 (2008) 810–817.
[30] N. Blouin, A. Michaud, M. Leclerc, A low-bandgap poly(2,7-carbazole) derivative for use in high-performance solar cells, Adv. Mater. 19 (2007) 2295–2300.
[31] G. Dennler, M.C. Scharber, C.J. Brabec, Polymer-fullerene bulk-heterojunction solar cells, Adv. Mater. 21 (2009) 1323–1338.
[32] V. Badescu, A.M. Badescu, Improved model for solar cells with up-conversion of low-energy photons, Renew. Energy 34 (2009) 1538–1544.